International Journal of Technology 11(4) 743-753 (2020)
Received July 2019 / Revised November 2019 / Accepted July 2020

International Journal of Technology

http://ijtech.eng.ui.ac.id

Investigation of Ground Motion and Local Site Characteristics of the 2018 Lombok Earthquake Sequence

Sigit Pramono[1,2*], Widjojo A. Prakoso[2], Supriyanto Rohadi[1], Dwikorita Karnawati[1], Dadang Permana[1], Bambang S. Prayitno[1], Ariska Rudyanto[1], Muhamad Sadly[1], Artadi P. Sakti[1], Ardian Y. Octantyo[1]

[1]*Indonesian Agency for Meteorological, Climatological and Geophysics, Jakarta 10620, Indonesia*
[2]*Department of Civil Engineering, Faculty of Engineering, Universitas Indonesia, Kampus UI Depok, Depok 16424, Indonesia*

Abstract. In 2018, Lombok Island was hit by a major earthquake sequence. The Indonesia Meteorological, Climatological, and Geophysics Agency (BMKG) reported that the Lombok Island earthquake sequence started with an M_w 6.4 foreshock, followed by an M_w 6.8 main shock, aftershocks of M_w 5.8 and M_w 6.2, and a second mainshock of M_w 6.9 in the eastern part of Lombok. This study presents an investigation of strong motion characteristics using the Indonesia National Strong Motion Network (INSMN) data from two accelerometer stations, the MASE station (at Praya Lombok International Airport, Lombok Island, V_{s30} = 770 m/s, SB site class) and TWSI station (in Sumbawa Island, V_{s30} = 1152 m/s, SB site class). Signal analysis techniques using a power spectrum via fast Fourier transform, wavelet transform and horizontal-to-vertical spectral ratio (HVSR) have been applied in this study. There are significant differences in the results (e.g., predominant frequencies, wavelets, H/V ratios, and frequencies at peak H/V ratio) for the MASE and TWSI stations, highlighting the importance of actual V_{s30} profiles and the limitation of the site class system in providing necessary predictive information. The variation of the peak ground acceleration (PGA) values and the spectral amplitudes could only be explained by hypothesizing the effect of the volcanic structure of Mount Rinjani on the strong motion waveforms.

Keywords: Fourier transform; HVSR; Strong motion; Vs30; Wavelet

1. Introduction

The historical seismicity in Lombok shows that Lombok Island is an area of active seismicity. Historical destructive events with M >5 have occurred, e.g., May 30, 1979, M 6.1; January 2, 2004, M 6.2; June 22, 2013, M 5.4; and June 9, 2016, M 6.2. According to the Indonesia Meteorological, Climatological, and Geophysics Agency (BMKG) earthquake database, on July 1, 2018, the Lombok region was hit by an earthquake with a magnitude of 4.5. Then, on July 29 at 05:47:39 local time, Lombok Island was hit by an M_w 6.4 earthquake at a depth of 13 km. This was a destructive earthquake that caused many buildings to collapse and was felt by almost everyone on Lombok Island, significantly impacting the western Lombok area. The source mechanism identified from the moment tensor indicated a thrust fault mechanism.

*Corresponding author's email: wprakoso@eng.ui.ac.id, Tel.: +62-21-7270029; Fax: +62-21-7270028
doi: 10.14716/ijtech.v11i4.3302

BMKG earlier believed that this earthquake was a mainshock, but then on August 5, 2018, an M_w 6.8 earthquake struck Lombok Island. It was followed by a sequence of earthquakes with magnitudes of M_w 5.8 and M_w 6.2, as well as an M_w 6.9 mainshock in the eastern part of Lombok on August 19, 2018. It is noted that these magnitudes have been recalculated and are somewhat different from those stated in earlier publications (e.g., Supendi et al. 2020).

Figure 1 shows the distribution of relocated earthquake epicenters and depths, including the five largest events in the Lombok earthquake sequence. The distribution of aftershocks reflects the back thrust fault model in northern Lombok Island. The aftershocks had a similar mechanism to the first and second mainshocks, as indicated by the model of focal mechanisms in Figure 1. The depths of the earthquakes were consistently shallow.

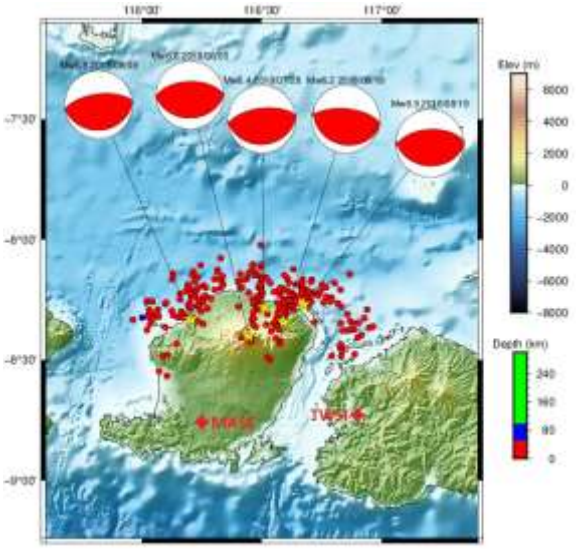

Figure 1 Seismicity of mainshocks and aftershocks of the Lombok earthquake sequence

This study presents an investigation into the characteristics of the strong ground motions of the Lombok earthquake sequence, with mainshocks of M_w 6.8 and M_w 6.9. These characteristics could be related to the potential damage to the buildings and other critical infrastructure on Lombok Island. The aim of the study is to examine the effects of local site characteristics on the strong motions of the Lombok earthquake sequence. The approach taken examines the strong motions recorded at BMKG stations with 1) the same site class and 2) similar distances from the sources. The site class considered is SB with an averaged shear-wave velocity to 30 m depth (V_{s30}) of 750 m/s to 1500 m/s (e.g., BSN 2019). The parameters considered include peak ground accelerations, energy amplitudes, wavelets, and predominant frequencies. The differences observed would lead to the hypothesis of the effect of Mount Rinjani on strong motions; the mountain is located south of the hypocenters. In this study, two stations were used to examine detailed characteristics of the ground motions. One station is the MASE station located in Lombok International Airport, while the other station is the TWSI station in Taliwang in the western part of Sumbawa Island, east of Lombok Island; the locations of these stations are shown in Figure 1.

1.1. Geological Setting

A geological map from the Center of Geological Survey of Indonesia reveals that the area around Mount Rinjani is within the Quaternary Period (Q_v), and that the other parts of Lombok Island are predominantly within the Tertiary Period (TI). The periods of these locations are shown in Figure 2a.

The frequent earthquakes in Indonesia are related to the convergence of the Pacific, Indo-Australian, and Eurasian plates. The Lombok area is active, as revealed by many seismotectonic studies. Volcano activities have also been frequently observed. Tectonically, Lombok Island is located in the inner arc of the Nusa Tenggara islands, which was formed by the Indo-Australian plate subducting under the Eurasian slab. This subduction is nearly arc–normal, with a dip angle between 60–70° and a crust thickness of about 20 km (Curray et al. 1977). The Wadati-Benioff zone extends to a depth of about 164 km (Rachmat et al. 2016).

Seismotectonically, Lombok Island is surrounded by four earthquake sources. South of Lombok Island, there is a subduction zone related with subduction activity from west of Sumatera and south of Java and Bali Island to the Timor Trough. In the northern part of Lombok Island, a back arc thrust source mechanism has been identified, the Bali Basin back arc thrust, and the Flores Thrust running from west to east. In the western and eastern parts of Lombok Island, faults (Lombok and Sumbawa faults) have also been identified (PUSGEN, 2017). According to the newly updated Indonesia Hazard Map, the maximum size of an earthquake on the back arc thrust is M_w 7.4.

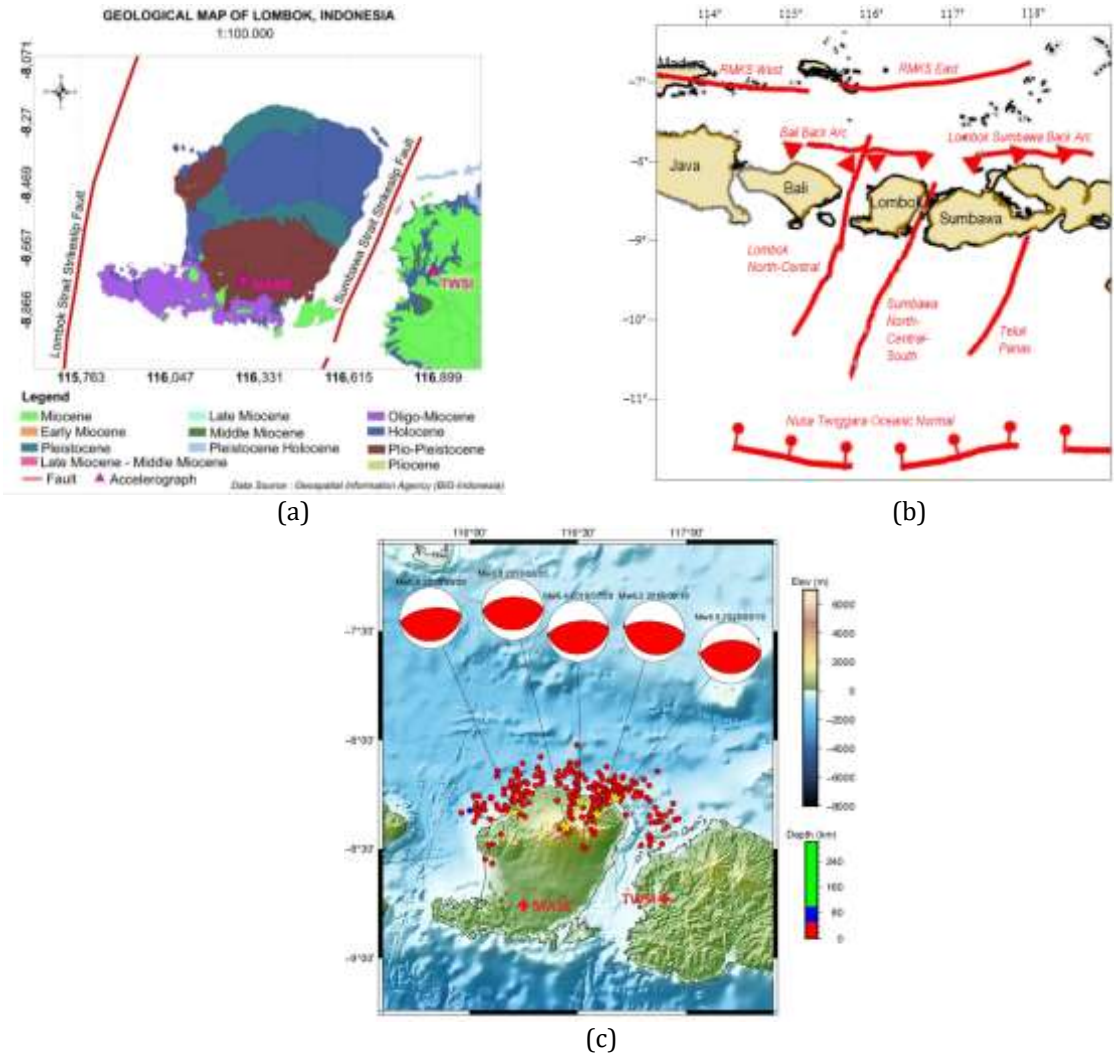

(a) (b)

(c)

Figure 2 (a) Geological map of Lombok Island; (b) Schematic seismic faults for Lombok (modified after PUSGEN, 2017); (c) V_{s30} profiles of the MASE and TWSI stations

1.2. V_{s30}-Based Site Classification

We conducted a local site investigation using the HVSR method with single microtremor measurements to obtain the predominant periods and the MASW method to obtain V_{s30} values for the MASE accelerometer station at Lombok International Airport and the TWSI accelerometer station in Taliwang, Sumbawa Island. Figure 2c shows the profiles of V_s (shear wave velocity) with depth. The weighted average of V_s over the top 30 meters (V_{s30}) is 770 m/s for the MASE station (Part of the MASW survey was reported in Krisnanto et al. (2018) and 1151 m/s for the TWSI station. Even though the actual V_s profiles are different, both were classified as site class SB (BSN, 2019). Therefore, other parameters are needed to explain the actual different responses when an earthquake occurs.

2. Methods

The strong motions that were recorded using a three-component accelerometer at the MASE and TWSI stations for the Lombok earthquake sequence and obtained from the BMKG data center were examined. Each data set was processed in the same way. First, we divided the total time window into a few seconds subwindows. Then, we processed the Fourier transform and smoothed it with a homogenous filter in log-scale (Konno and Ohmachi, 1998) and evaluated the horizontal-to-vertical spectral ratio (HVSR). It is noted that some previous studies showed that the presence of a large amplitude HVSR peak is related to a high impedance contrast between the sedimentary cover and the basement (Bard 1999; Bonnefoy-Claudet et al., 2006; Bonnefoy-Claudet et al., 2009), while a low amplitude peak is related to a lower contrast, indicating the presence of a hard soil (Woolery and Street 2002; Bonnefoy-Claudet et al., 2006; Bonnefoy-Claudet et al., 2009). It is noted that recent studies on the effects of local site characteristics on strong motions include Seyhan and Stewart (2014), Borcherdt (2015), Ji et al. (2017), Pramono et al. (2017), Prakoso et al. (2017), as well as Mase (2018).

A major geologic feature in Lombok Island is the volcano Mount Rinjani. The effect of volcanic structures on strong motion attenuation has been recognized in the literature (e.g., Ghofrani and Atkinson 2011). These structures typically have low seismic velocity and filter out the high-frequency content of propagating motions.

2.1. Data Sets

2.1.1. Strong motion data

The data used in this study were recorded by accelerometers within the Indonesia National Strong Motion Network, namely from the BIL (Lombok International Airport) station in Lombok Island called MASE and the Taliwang station in Sumbawa Island called TWSI. The earthquake parameters are summarized in Table 1.

Figure 3 shows a strong motion waveform for the M_w 6.9 earthquake event at the MASE and TWSI stations (Detailed variations of strong motions for other events at the MASE and TWSI stations are presented in the Supplementary Figures). Note that, in Figure 3, the acceleration scale for the MASE station is 1/20 of that for the TWSI station. The path from the epicenter to the MASE station would pass Mount Rinjani, while that to the TWSI station would be a direct path. In addition, a visual comparison of the MASE and TWSI station waveforms suggests that the MASE station waveform tends to have lower frequencies relative to the TWSI station waveform. This is in general related to the fact that, although both belong to site class SB, the V_{s30} of the MASE station is lower than that of the TWSI station, highlighting the effects of local site characteristics on the strong motions. It should be noted that the difference in the acceleration scale varies for each event, while that of the MASE station waveforms tends to have lower frequencies for all events.

Table 1 Significant Lombok earthquake (Source: BMKG, 2018)

Date	OT (UTC)	Lat (°S)	Long (°BT)	Depth (Km)	Mag. (M_w)
July 28, 2018	22:47:39	8.35	116.50	13	6.4
August 5, 2018	11:46:35	8.35	116.47	32	6.8
August 9, 2018	05:25:32	8.44	116.21	14	5.8
August 19, 2018	04:10:23	8.44	116.59	18	6.2
August 19, 2018	14:56:27	8.37	116.70	18	6.9

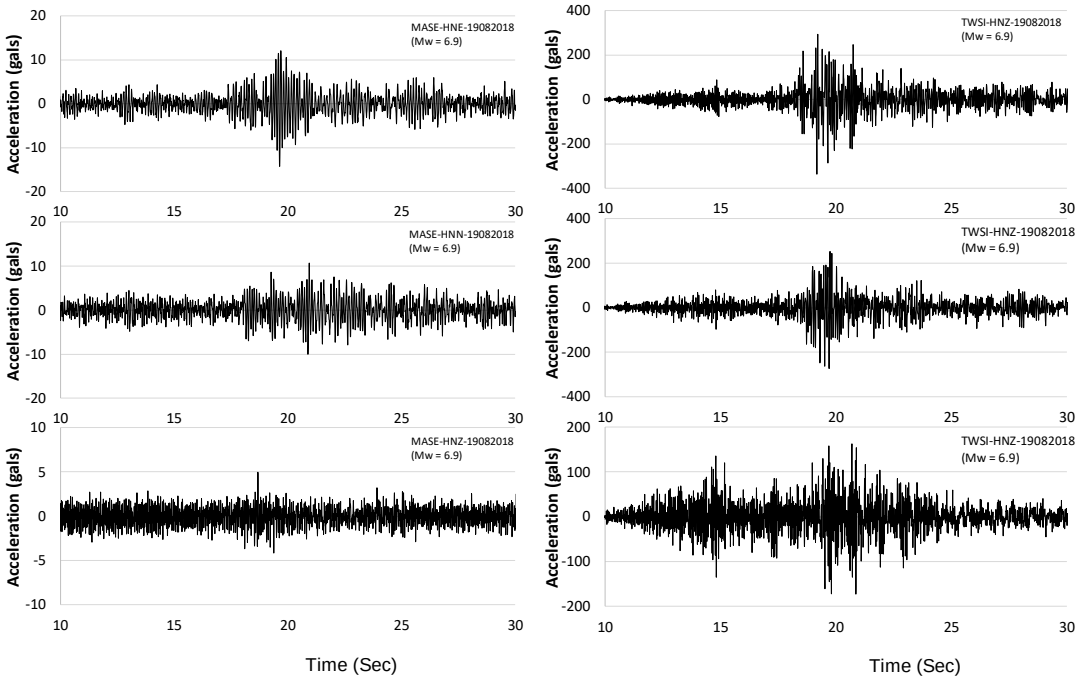

Figure 3 Strong motion waveforms of the MASE and TWSI stations for M_w 6.9 earthquake

The peak ground acceleration (PGA) values of all considered events are summarized in Tables 2 and 3 for the MASE and TWSI stations, respectively. For M_w 6.8 and M_w 5.8, the PGA values of the MASE station are greater (ratio about 1.6 to 3.0 for M_w 6.8 and ratio about 2.1 to 3.1 for M_w 5.8) than those of the TWSI station, as the distances from the sources to the MASE station were less than the distances to the TWSI station; this is consistent with the theoretical wave geometrical damping. However, for M_w 6.4, the PGA values of the MASE station are much smaller (ratio about 14% to 20%) than those of the TWSI station, although the distance from the source to the MASE station was less than the distance to the TWSI station. For M_w 6.2, the PGA values of the MASE station are again much smaller (ratio about 4% to 11%) than those of the TWSI station, although the distance from the source to both stations is about the same. For M_w 6.9, the PGA values of the MASE station are much smaller (ratio about 3% to 4%) than those of the TWSI station. It is noted that the latter could be only partially explained by the theoretical wave geometrical damping, as the ratio is very significant. These inconsistent PGA values suggest that there is a major waveform modifier along the paths from the epicenter to both stations; it is suggested that the modifier is the volcanic structure of Mount Rinjani.

Tables 2 and 3 also show the peak period of the HVSR T_g. For the MASE station, the range of T_g is 0.112 to 0.118 seconds, while that for the TWSI station is 0.058 to 0.064 seconds. The ranges are relatively consistent with the V_{s30} values for both locations (e.g., Ji et al., 2017).

Table 2 PGA records at the MASE station (V_{S30} = 771 m/s, Site Class SB) for each earthquake event

Magnitude (M_w)	Distance (km)	PGA (gals)			$T_{g\,(HVSR)}$ (s)
		E	N	Z	
6.4	42.2	5.655	6.217	3.034	0.11781
6.8	48.7	30.476	44.331	18.241	0.11781
5.8	37.1	34.183	29.298	13.626	0.11532
6.2	43.6	3.142	5.429	1.937	0.11286
6.9	43.9	12.066	10.026	4.968	0.11497

Table 3 PGA records at the TWSI station (V_{S30} = 1151 m/s, Site Class SB) for each earthquake event

Magnitude (M_w)	Distance (km)	PGA (gals)			$T_{g\,(HVSR)}$ (s)
		E	N	Z	
6.4	55.9	41.309	30.698	15.786	0.05884
6.8	58.5	18.890	14.437	11.115	0.05789
5.8	79.6	13.963	9.190	6.498	0.05741
6.2	44.5	54.311	48.137	51.481	0.05669
6.9	32.3	252.595	293.208	172.871	0.06363

2.1.2. Investigation methods

It has been shown that PGA alone could not explain the strong motion waveforms of the Lombok earthquake sequence. The strong motions recorded by the MASE and TWSI stations are examined further by performing the frequency domain analysis using a fast Fourier transform (FFT), wavelet analysis, and HVSR spectral ratio analysis. The results are then discussed in the context of the major geologic features on Lombok Island, as well as the differences in V_{s30} values at both stations.

3. Results and Discussion

3.1. Earthquake Characteristics in Frequency Domain

The FFT analysis results of the three-component waveforms for the M_w 6.9 event are shown in Figure 4 for both the MASE and TWSI stations; those for other events are shown in the Appendix. The spectral amplitudes for the MASE station are much lower than those for the TWSI station, indicating that the motion recorded at the MASE station is much lower than that at the TWSI station. It should be noted that this is not the case for the other events. As previously discussed, this variation in spectral amplitudes is due to effects of the major geologic feature, the actual V_{s30} profiles, and the distance between the epicenter and the recording stations.

Figure 4 shows that the predominant frequencies of the spectrum of the MASE station are lower than those of the TWSI station, consistent with the actual V_{s30} profiles; this observation is also true for the other events, as shown in the Appendix. Table 4 summarizes the predominant frequencies for all considered events recorded by both stations. The predominant frequency of the horizontal components for the MASE station varied from 7.97 Hz to 9.0 Hz, while that of the vertical component for the MASE station varied from 2.1 Hz to 3.9 Hz, with the exception of 16.2 Hz for M_w 6.9. This exception may be related to the motion recorded at the MASE station being very low. The predominant frequency of the horizontal components for the TWSI station varied from 15.71 Hz to 19.17 Hz, while the predominant frequency of the vertical component for the TWSI station ranged from 21.15

Hz to 29.48 Hz. In general, the predominant frequencies of the strong motions from the TWSI station are higher than those from the MASE station, which is consistent with the actual V_{s30} profiles in the same SB site class.

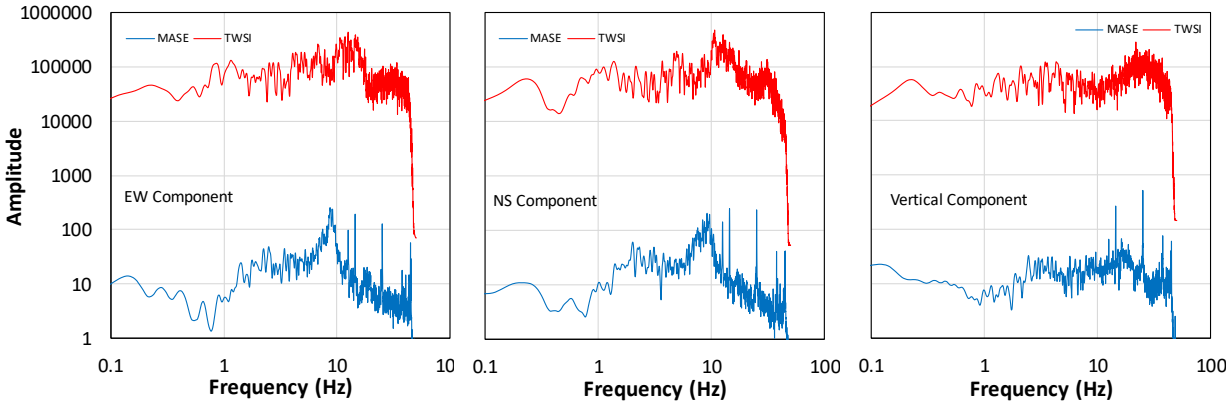

Figure 4 FFT results of Mw 6.9 strong motions for the MASE (blue) and TWSI stations (red)

Table 4 Predominant frequencies for each earthquake event for the MASE and TWSI stations

	M_w 6.4			M_w 6.8			M_w 5.8			M_w 6.2			M_w 6.9		
MASE	EW (Hz)	NS (Hz)	Z (Hz)	EW (Hz)	NS (Hz)	Z (Hz)	EW (Hz)	NS (Hz)	Z (Hz)	EW (Hz)	NS (Hz)	Z (Hz)	EW (Hz)	NS (Hz)	Z (Hz)
	8.86	8.33	2.36	8.26	8.08	2.63	8.50	8.53	3.87	8.41	7.97	2.16	8.63	9.00	16.2
	M_w 6.4			M_w 6.8			M_w 5.8			M_w 6.2			M_w 6.9		
TWSI	EW (Hz)	NS (Hz)	Z (Hz)	EW (Hz)	NS (Hz)	Z (Hz)	EW (Hz)	NS (Hz)	Z (Hz)	EW (Hz)	NS (Hz)	Z (Hz)	EW (Hz)	NS (Hz)	Z (Hz)
	17.90	15.96	29.08	18.28	16.32	29.48	19.17	16.1	22.93	17.16	15.71	21.50	12.46	10.63	21.7

3.2. Wavelet Analysis

To analyze the variation in the frequency contents of the waveforms over time, a wavelet analysis for each waveform was performed. Figure 5 shows the results of the wavelet analyses for the M_w 6.9 event. The color change from red to magenta is the gradation from low to high energy.

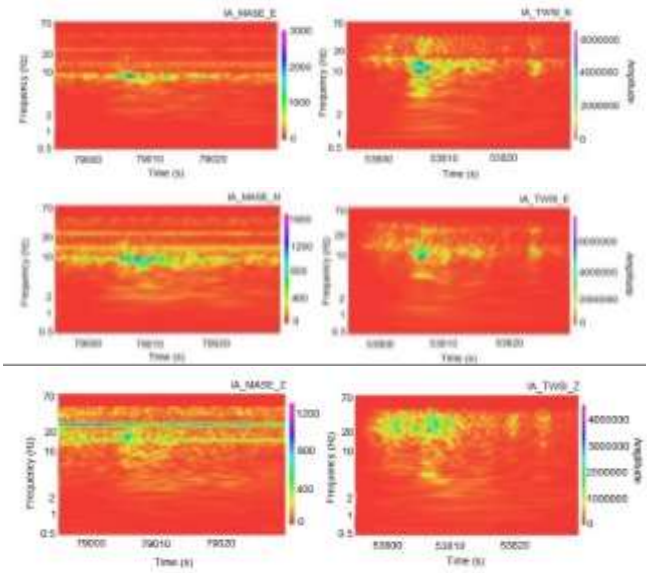

Figure 5 Results of wavelet analysis for Mw 6.9 of the MASE (left) and TWSI stations (right)

Table 5 summarizes the variations of wavelet values related with the time history and frequency content for the MASE station. The frequency at wavelet maximum energy should be associated with the predominant frequency from the accelerometer signal. As can be seen, the maximum energy of horizontal signals occurred at higher frequencies compared to that of the vertical signals, except for the last earthquake, M_w 6.9. The trend of times for maximum energy of the horizontal and vertical signals is similar for all earthquakes.

Table 6 summarizes the variation of wavelet values related with the time history and the frequency contents for TWSI station signals. As can be seen, the maximum energy of the horizontal signals occurred at lower frequencies compared to that of the vertical signals. The maximum energy of the horizontal signals tended to occur at earlier or similar times as that of the vertical signals. The difference in observed wavelets is consistent with the measured V_{s30} difference, although both stations are site class SB.

Table 5 Maximum energy by wavelet analysis of the MASE station for each earthquake event

M_w 6.4			M_w 6.8			M_w 5.8		
EW (Hz)	NS (Hz)	Z (Hz)	EW (Hz)	NS (Hz)	Z (Hz)	EW (Hz)	NS (Hz)	Z (Hz)
Max Energy Wavelet (Hz)								
1-10 9	1-10 9	1-20 2.5	5-10 9	5-10 9	1-20 2.5	5-10 9	5-10 9	1-20 4
M_w 6.2			M_w 6.9					
EW (Hz)	NS (Hz)	Z (Hz)	EW (Hz)	NS (Hz)	Z (Hz)			
Max Energy Wavelet (Hz)								
1-10 9	1-10 8	1-20 3	5-10 9	5-10 9	10-24 24			

Table 6 Maximum energy by wavelet analysis of the TWSI station for each earthquake event

M_w 6.4			M_w 6.8			M_w 5.8		
EW (Hz)	NS (Hz)	Z (Hz)	EW (Hz)	NS (Hz)	Z (Hz)	EW (Hz)	NS (Hz)	Z (Hz)
Max Energy Wavelet (Hz)								
10-20 16	10-20 16	10-50 25	10-20 18	10-20 16	10-50 24	5-20 18	5-20 18	10-50 25
M_w 6.2			M_w 6.9					
EW (Hz)	NS (Hz)	Z (Hz)	EW (Hz)	NS (Hz)	Z (Hz)			
Max Energy Wavelet (Hz)								
5-20 18	5-20 18	10-50 22	5-20 10	5-20 10	10-50 24			

3.3. HVSR Spectral Ratio

We also conducted a HVSR analysis to provide additional characterizations of the Lombok earthquake sequence. The HVSR ratios were obtained to provide the predominant period or the predominant frequency of the site and might explain the observed responses when an earthquake occurs. Figure 6 shows the M_w 6.9 H/V ratio graphs for the MASE and TWSI stations; the graphs for other events are shown in the Appendix.

Table 7 show the HVSR results for the five events. For each station, the HVSR spectras are relatively consistent. The predominant frequencies for the MASE station varied from 8.4 hz to 8.86 hz with a deviation of 0.25 to 0.47 hz, while the predominant frequencies for the TWSI station varied from 15.72 to 17.64 hz with a deviation of 0.36 to 0.9. It is noted that the difference in predominant frequencies is consistent with the measured V_{s30} difference, although both stations are site class SB.

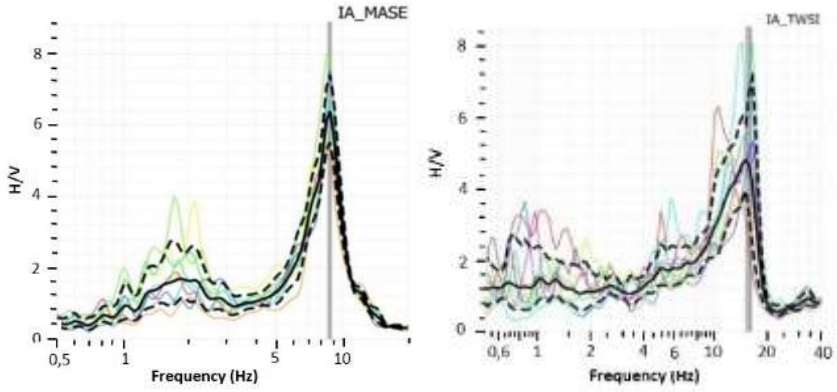

Figure 6 HVSR spectra of M_w 6.9 earthquake event for the MASE and TWSI stations

Table 7 HVSR analysis results for the predominant frequency at the MASE and TWSI stations for each event

Magnitude	Predominant Frequency ± SD	
M_w	MASE	TWSI
6.4	8.67 ± 0.36	16.56 ± 0.36
6.8	8.48 ± 0.47	17.27 ± 0.65
5.8	8.67 ± 0.35	17.64 ± 0.91
6.2	8.86 ± 0.25	17.64 ± 0.91
6.9	8.69 ± 0.35	15.72 ± 0.68

The H/V ratio for the MASE station tended to be higher than the H/V ratio for the TWSI station. For the former, the range is between 6 and 8, while for the latter, the range is between 4 and 6. It is noted that the difference in H/V ratios is consistent with the measured V_{s30} difference (e.g., Ji et al. 2017).

The HVSR spectra for the MASE station show a secondary peak at a frequency of about 1 Hz to 2 Hz, and the H/V ratio is about 1 to 3. This indicates that there may be a layer with low velocity within the MASE station.

4. Conclusions

We examined the strong motions of the Lombok earthquake sequence by considering two stations located in sites of the same site class. The stations have V_{s30} values of 770 m/s (MASE) and 1151 m/s (TWSI). Five earthquakes in the sequence were considered. We performed a fast Fourier transform analysis, wavelet analysis, and HVSR analysis. In general, the predominant frequency of strong motions from the MASE station are lower than those from the TWSI station. For the MASE station, the maximum energy of horizontal signals typically occurred at higher frequencies compared to that of the vertical signals, and the time trend for the maximum energy of the horizontal and vertical signals is similar for all earthquakes. For the TWSI station, the maximum wavelet energy of the horizontal signals occurred at lower frequencies compared to that of the vertical signals, and the maximum wavelet energy of the horizontal signals tended to occur at earlier or similar times as that of the vertical signals. Moreover, the H/V ratio for the MASE station tended to be lower than the ratio for the TWSI station. It is highlighted therefore that differences in measured V_{s30} can cause different earthquake strong motions and that the site class system might not provide all necessary predictive information. The variation of the peak ground

acceleration (PGA) values and the spectral amplitudes could only be partially explained by the theoretical wave geometrical damping. This suggests that there is a major waveform modifier along the paths from the epicenter to both stations; it is hypothesized that the modifier is the volcanic structure of Mount Rinjani, a major geologic feature of Lombok Island.

Acknowledgements

We would like to gratefully thank the support for this study provided by the Indonesian Agency for Meteorological, Climatological and Geophysics (BMKG), as well as a Kemenristekdikti PTUPT Research Grant (Universitas Indonesia Contract No. 120/SP2H/PTNBH/DRPM/2018).

References

Badan Standarisasi Nasional (BSN), 2019. SNI 1726:2019. *Tata Cara Perencanaan Ketahanan Gempa Untuk Bangunan Gedung dan Non Gedung*, (Earthquake Resistant Design Codes for Buildings and Non-buildings), Jakarta

Bard, P.Y., 1999. Microtremors Measurements: A Tool for Site Effect Estimation? *In*: Proceedings the Effects of Surface Geology on Seismic Motion, Volume 3. Rotterdam, Balkema, pp. 1251–1279

Bonnefoy-Claudet, S., Cornou, C., Bard, P.Y., Cotton, F., Moczo, P., Kristek, J., Fäh, D., 2006. H/V Ratio: A Tool for Site Effects Evaluation. Results From 1-D Noise Simulations. *Geophysical Journal International*, Volume 167(2), pp. 827–837

Bonnefoy-Claudet, S., Baize, S., Bonilla, L.F., Berge-Thierry, C., Pasten, C., Campos, J., Volant, P., Verdugo, R., 2009. Site Effect Evaluation in the Basin of Santiago de Chile using Ambient Noise Measurements. *Geophysical Journal International*, Volume 176(3), pp. 925–937

Borcherdt, R.D., 2015. NGA-West2 GMPE Average Site Coefficients for Use in Earthquake-Resistant Design, USGS Open-File Report, pp. 2015–1116

Curray, J.R., Shor, G.G., Raitt, R.W., Henry, M., 1977. Seismic Refraction and Reflection Studies of Crustal Structure of the Eastern Sunda and Western Banda Arcs. *Journal of Geophysics Research*, Volume 82(17), pp. 2479–2489

Ghofrani, H., Atkinson, G.M., 2011. Forearc versus Backarc Attenuation of Earthquake Ground Motion. *Bulletin of the Seismological Society of America*, Volume 101(6), pp. 3032–3045

Ji, K., Ren, Y., Wen, R., 2017. Site Classification for National Strong Motion Observation Network System (NSMONS) Stations in China using an Empirical H/V Spectral Ratio Method. *Journal of Asian Earth Sciences*, Volume 147, pp. 79–94

Konno, K., Ohmachi, T., 1998. Ground-motion Characteristics Estimated from Spectral Ratio between Horizontal and Vertical Components of Microtremor. *Bulletin of the Seismological Society of America*, Volume 88(1), pp. 228–241

Krisnanto, S., Irsyam, M, Asrurifak, M., Alatas, M.I., Adi, A.D., Darjanto, H., Prakoso, W.A., Pramono, S., 2018. Aspek Geoteknik dan Seismic Hazard. Kajian Rangkaian Gempa Lombok, Provinsi Nusa Tenggara Barat, Indonesia (*Geotechnical Aspects and Seismic Hazard. Study of the Series of Earthquakes in Lombok, West Nusa Tenggara Province, Indonesia*). Research Institute for Housing and Human Settlements, Ministry of Public Works and Housing, Republic of Indonesia

Mase, L.Z., 2018, Reliability Study of Spectral Acceleration Designs Against Earthquakes in Bengkulu City, Indonesia, 2018. *International Journal of Technology*, Volume 9(5), pp. 910–924

National Center for Earthquake Studies of Indonesia (PUSGEN), 2017. *Seismic Sources and Hazard Maps for Indonesia*. Research Institute for Housing and Human Settlements, Ministry of Public Works and Housing, Republic of Indonesia

Prakoso, W.A., Rahayu, A., Sadisun, I.A., Muntohar, A.S., Muzli, M., Rudyanto, A., 2017. Comparing Shear-wave Velocity Determined by MASW with Borehole Measurement at Merapi Sediment in Yogyakarta. *International Journal of Technology,* Volume 8(6), pp. 993–1000

Pramono, S., Prakoso, W.A., Cummins, P., Rahayu, A., Rudyanto, A., Syukur, F., Sofian, 2017. Investigation of Subsurface Characteristics by using a Vs30 Parameter and a Combination of the HVSR and SPAC Methods for Microtremor Arrays. *International Journal of Technology*, Volume 8(6), pp. 983–992

Rachmat, H., Rosana, M.F., Wirakusumah, A.D., Jabbar, G.A., 2016. Petrogenesis of Rinjani Post-1257-Caldera-Forming-Eruption Lava Flows. *Indonesian Journal on Geoscience*, Volume 3(2), pp. 107–126

Seyhan, E., Steward, J.P., 2014. Semi-empirical Nonlinear Site Amplification from NGA-West2 Data and Simulations. *Earthquake Spectra*, Volume 30(3), pp. 1241–1256

Supendi, P., Nugraha, A.D., Widiyantoro, S., Pesicek, J.D., Thurber, C.H., Abdullah, C.I., Daryono, D., Wiyono, S.H., Shiddiqi, H.A., Rosalia, S., 2020. Relocated Aftershocks and Background Seismicity in Eastern Indonesia Shed Light on the 2018 Lombok and Palu Earthquake Sequences. *Geophysical Journal International*, Volume 221(3), pp. 1845–1855

Woolery, E.W., Street, R., 2002. 3D Near-surface Soil Response From H/V Ambient-noise Ratios. *Soil Dynamics and Earthquake Engineering*, Volume 22(9-12), pp. 865–876